JOURNAL OF THERMOPHYSICS AND HEAT TRANSFER
Vol. 27, No. 3, July–September 2013

# Performance Analysis of Irreversible Miller Cycle Under Variable Compression Ratio

Rahim Ebrahimi* and Marzie Hoseinpour†
*Shahrekord University, Shahrekord, Iran*

DOI: 10.2514/1.T3981

**The recent improvements on spark ignition engines have been the result of improved engine thermodynamic cycles, made possible by advances in technologies such as variable valve timing, variable compression ratio, and turbines of variable geometry. To assess the improvement capability of engine performance under a changing thermodynamic cycle, performance of an irreversible Miller cycle in internal combustion engines is analyzed using finite time thermodynamics. In this model, the nonlinear relation between the specific heats of a working fluid and its temperature, the frictional loss computed according to the mean velocity of the piston, and heat transfer loss through the cylinder wall are considered. The relations between the power output and the compression ratio and between the thermal efficiency and the compression ratio are indicated by detailed numerical examples. Moreover, the effects of variation of combustion chamber volume and variation of piston displacement volume on the cycle performance are analyzed. The results obtained herein have realistic significance and may provide guidelines for the design and evaluation of practical internal combustion engines.**



## Introduction

RECENT engine developments are being made mainly by friction reduction, combustion improvement, and thermodynamic cycle modification. New technologies such as variable valve timing or variable compression ratio are used for the thermodynamic improvement of internal combustion engines and are important for the latter. To evaluate the potential for thermodynamic improvement of these and other technologies, numerical studies must be performed using different tools [1–3].

In the last three decades, finite time thermodynamics (FTT) has been developed [4–8]. This approach consists of an extension of classical equilibrium thermodynamics by the inclusion of some classes of irreversibilities in the thermodynamic formalism. FTT is a powerful tool for the performance analysis and optimization of real engine cycles [9,10]. Such models are used for comparison reasons to show the effect of varying engine parameters, conditions, fluid properties, etc. Meanwhile, good approximations of power output, thermal efficiency, and mean effective pressure can be expected [11]. Several studies have examined the finite time thermodynamic performance of reciprocating heat engines. Klein [12] studied the effect of heat transfer through a cylinder wall on the work output of the Otto and Diesel cycles. Angulo-Brown et al. [13] derived the compression ratio of an optimized air standard Otto cycle model with friction-like loss during a finite time. Al-Sarkhi et al. [14] studied the effect of maximizing power density on the cycle efficiency for the Miller cycle without any loss and compared them with those of the Atkinson and Joule–Brayton cycles by using numerical examples. Hou [15] investigated the effect of heat transfer through the cylinder wall on the performance of a dual cycle. Zhao and Chen [16] performed analysis and parametric optimum criteria of an irreversible Miller heat engine using finite time thermodynamics. The performance of the cycle is optimized with respect to the pressure ratio of the working substances. Ge et al. [17] analyzed a model of air standard Otto cycle using finite time thermodynamics and outlined effects of heat transfer, friction, and internal irreversibility on the performance of cycle. Al-Sarkhi et al. [18] evaluated the performance of the Miller cycle under different specific heat models (i.e., constant, linear, and polynomial) for the air. Wang et al. [19,20] investigated the application of the Miller cycle concept, both analytically and experimentally to reduce engine exhaust gas emissions. Chen et al. [21] described a class of generalized irreversible reciprocating heat engines. The cycle model consisted of two heating branches, two cooling branches, and two adiabatic branches with consideration of the losses of heat transfer, friction, internal irreversibility, and variable specific heat. Lin and Hou [22] investigated the effects of friction and variable specific heats of the working fluid and heat loss as characterized by a percentage of the fuel's energy on the performance of an air standard Miller cycle under the restriction of the maximum cycle temperature. Ebrahimi [23] analyzed effects of the variable specific heat ratio of working fluid on the performance of Diesel cycles. Ebrahimi [24] investigated effects of mean piston speed, equivalence ratio, and cylinder wall temperature on the performance of an Atkinson engine by using numerical examples.

The Miller cycle engine was patented by an American engineer, Ralph Miller in 1947 [25]. The main difference between the Miller cycle engine and a common (Otto cycle) automobile engine is that the former has a longer expansion stroke, while retaining a shorter compression stroke. This is accomplished by closing the intake valve before the termination of the intake stroke or keeping the intake valve open during a portion of the compression stroke [11]. The Miller cycle can be applied to an internal combustion engine using variable valve timing. A significant improvement to the Miller cycle may be achieved if compression ratio adjustment is used in addition to valve timing variation [26,27].

As can be seen in the relevant literature, the investigation of the effect of the variation of combustion chamber volume and the variation of piston displacement volume on performance of the Miller cycle does not appear to have been published. Therefore, the objective of this study is to evaluate the effects of the variation of combustion chamber volume and the variation of piston displacement volume on the performance of the Miller cycle.

Received 5 July 2012; revision received 21 December 2012; accepted for publication 10 January 2013; published online 17 May 2013. 

*Department of Agriculture Machine Mechanics, P.O. Box 115; Rahim.Ebrahimi@gmail.com. (Corresponding Author).

†Department of Agriculture Machine Mechanics, P.O. Box 115.

## Miller Cycle

The characteristic of the Miller cycle is that the effective compression stroke of the engine is shorter than the expansion stroke. Figure 1 shows the pressure–volume diagram of the Miller cycle. In this figure, different cases of the Miller cycle are shown assuming variation of combustion chamber volume and variation of piston displacement volume, in which the variation of the combustion chamber and piston displacement volumes are achieved through the

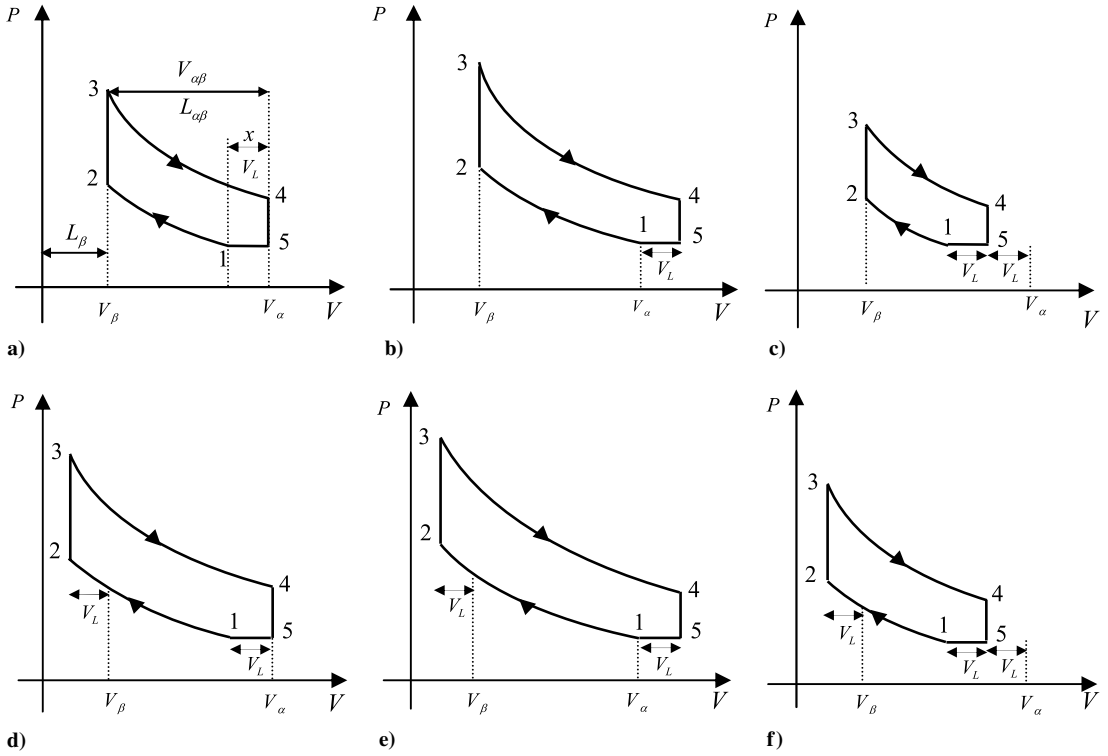


**Fig. 1 Pressure–volume diagram for the six cases of the Miller cycle.**



change of position of bottom dead center (BDC) and top dead center (TDC). It should be noted here that the other cases are similar to these six cases.

The mass flow rate of air is calculated as [28]

$$\dot{m}_a = \frac{\eta_v \rho_a V_d N}{2} \tag{1}$$

where $\dot{m}_a$ is the mass flow rate of air, $V_d$ is the piston displacement volume, $\rho_a$ is air density, and $N$ is the engine speed. The relations between $\dot{m}_a$ and the mass flow rate of fuel $\dot{m}_f$, and between $\dot{m}_a$ and the mass flow rate of the air–fuel mixture $\dot{m}_{\text{mix}}$, are defined as [28]

$$\dot{m}_f = \frac{\dot{m}_a \varphi}{\text{AF}_s} \tag{2}$$

and

$$\dot{m}_{\text{mix}} = \dot{m}_a \left(1 + \frac{\varphi}{\text{AF}_s}\right) \tag{3}$$

where $\varphi$ is the equivalence ratio, and $\text{AF}_s$ is the stoichiometric air–fuel ratio. It should be noted that the equivalence ratio is the ratio of the actual fuel/air ratio to the stoichiometric ratio (or its inverse).

The specific heat at constant pressure for the air–fuel mixture can be computed as [29]

$$C_{P\text{mix}} = C_{Pa} x_a + C_{Pf} x_f \tag{4}$$

where $C_{Pa}$ and $C_{Pf}$ are air specific heat and fuel specific heat, and $x_a$ and $x_f$ are the mass fractions for air and fuel, given, respectively, as

$$x_f = \frac{1}{1 + (\text{AF}_s/\varphi)} \tag{5}$$

$$x_a = 1 - x_f \tag{6}$$

According to the relation between $C_V$ and $C_P$, the specific heat at constant volume can be written as

$$C_{V\text{mix}} = C_{P\text{mix}} - R_{\text{mix}} \tag{7}$$

where $C_{V\text{mix}}$ is the specific heat of the air–fuel mixture at constant volume, and $R_{\text{mix}}$ is the gas constant for the mixture. It is calculated as follows [30]:

$$R_{\text{mix}} = \frac{R}{M_{\text{mix}}} \tag{8}$$

where $R$ is the gas constant of the air, and $M_{\text{mix}}$ is the molar mass of the mixture and is determined as

$$M_{\text{mix}} = M_a y_a + M_f y_f \tag{9}$$

where $M_a$ and $M_f$ are the molar mass of air and fuel, respectively, and $y_a$ and $y_f$ are the molar fractions of air and fuel, respectively, and are obtained as

$$y_f = \frac{1}{1 + 4.76(a_s/\varphi)} \tag{10}$$

$$y_a = 1 - y_f \tag{11}$$

where $a_s$ is the stoichiometric number of moles for the air.

The specific heat of the working fluid depends upon its temperature and this will influence the performance of the cycle. Over the temperature range from 200 to 6000 K, the specific heat curve is assumed to follow fourth-order polynomials, introduced by a team of researchers called the NASA polynomial equation [31]. According to data obtained from polynomials in [31], it can be assumed that the specific heat of both gasoline and air is the following third-order polynomial for the temperature range 300–2500 K:

$$C_{Pa} = 0.913 + 0.00T - 5.941 \times 10^{-8} T^2 + 1.909 \times 10^{-12} T^3 \tag{12}$$

$$C_{Pf} = 0.169 + 0.006T - 2.759 \times 10^{-6} T^2 + 4.643 \times 10^{-10} T^3 \tag{13}$$

In these relations, $T$ is temperature. Substituting Eqs. (5), (6), (12), and (13) into Eq. (4) yields $C_{P_{\text{mix}}}$ as follows:

$$C_{P\mathrm{mix}} = \frac{1}{\varphi + \mathrm{AF}_s}[0.169\varphi + 0.913\mathrm{AF}_s + 0.006\varphi T - (2.759\times10^{-6}\varphi + 5.941\times10^{-8}\mathrm{AF}_s)T^2 + (4.643\times10^{-10}\varphi + 1.909\times10^{-12}\mathrm{AF}_s)T^3] \quad (14)$$

For the constant volume heat addition process $2 \rightarrow 3$, the rate of heat transferred to the working fluid during the process $2 \rightarrow 3$ can be given as

$$\dot{Q}_{\mathrm{in}} = \dot{m}_{\mathrm{mix}}\int_{T_2}^{T_3}(C_{P\mathrm{mix}} - R_{\mathrm{mix}})\,\mathrm{d}T = \frac{\eta_v\rho_{\mathrm{air}}V_dN}{2}\left(\frac{1+\varphi}{\mathrm{AF}_s}\right)\left\{\frac{1}{\varphi+\mathrm{AF}_s}[0.003\varphi(T_3^2 - T_2^2) - (0.916\times10^{-6}\varphi + 1.980\times10^{-8}\mathrm{AF}_s)(T_3^3 - T_2^3) + (1.160\times10^{-10}\varphi + 0.477\times10^{-12}\mathrm{AF}_s)(T_3^4 - T_2^4) + (0.169\varphi + 0.913\mathrm{AF}_s)(T_3 - T_2)] - \frac{R(\varphi + 4.76a_s)(T_3 - T_2)}{\varphi M_f + M_a 4.76a_s}\right\} \quad (15)$$

The heat rejected per second by the working fluid during processes $4 \rightarrow 5$ and $5 \rightarrow 1$ is

$$\dot{Q}_{\mathrm{out}} = \dot{m}_{\mathrm{mix}}\left(\int_{T_4}^{T_5}(C_{P\mathrm{mix}} - R_{\mathrm{mix}})\,\mathrm{d}T + \int_{T_5}^{T_1} C_{P\mathrm{mix}}\,\mathrm{d}T\right) = \frac{\eta_v\rho_{\mathrm{air}}V_dN}{2}\left(\frac{1+\varphi}{\mathrm{AF}_s}\right)\left\{\frac{1}{\varphi+\mathrm{AF}_s}[0.003\varphi(T_1^2 - T_4^2) - (0.916\times10^{-6}\varphi - 1.980\times10^{-8}\mathrm{AF}_s)(T_1^3 - T_4^3) + (1.160\times10^{-10}\varphi + 0.477\times10^{-12}\mathrm{AF}_s)(T_1^4 - T_4^4) + (0.169\varphi + 0.913\mathrm{AF}_s)(T_1 - T_4)] - \frac{R(\varphi + 4.76a_s)(T_5 - T_4)}{\varphi M_f + M_a 4.76a_s}\right\} \quad (16)$$

Because $C_P$ and $C_V$ are dependent on temperature, the equation often used for a reversible adiabatic process with constant $C_V$ cannot be used for an adiabatic process with a variable $\gamma$ [18,32,33]. In the present work, the equation for the entropy change of an ideal gas [i.e., Eq. (17)] has been used to find relations between temperatures at various points in the cycle:

$$\Delta S = C_v\frac{\mathrm{d}T}{T} + R\frac{\mathrm{d}V}{V} \quad \text{or} \quad \Delta S = C_P\frac{\mathrm{d}T}{T} + R\frac{\mathrm{d}P}{P} \quad (17)$$

During the isentropic processes $1 \rightarrow 2$ and $3 \rightarrow 4$, Eq. (17) will be used to get a relation between $T_1$ and $T_2$ and another one between $T_3$ and $T_4$. Therefore, after substituting the value for $C_{V\mathrm{mix}}$ from Eq. (7) and performing the integration of Eq. (17), equations describing processes $1 \rightarrow 2$ and $3 \rightarrow 4$ can be, respectively, expressed as follows:

$$\frac{1}{\varphi+\mathrm{AF}_s}\left[(0.169\varphi + 0.913\mathrm{AF}_s)\ln\left(\frac{T_2}{T_1}\right) + 0.006\varphi(T_2 - T_1) - (1.379\times10^{-6}\varphi - 2.970\times10^{-8}\mathrm{AF}_s)(T_2^2 - T_1^2) + (1.547\times10^{-10}\varphi + 0.636\times10^{-12}\mathrm{AF}_s)(T_2^3 - T_1^3)\right] - \frac{R(\varphi + 4.76a_s)}{\varphi M_f + M_a 4.76a_s}\left[\ln\left(\frac{T_2}{T_1}\right) + \ln(r_c^*)\right] = 0 \quad (18)$$

$$\frac{1}{\varphi+\mathrm{AF}_s}\left[(0.169\varphi + 0.913\mathrm{AF}_s)\ln\left(\frac{T_4}{T_3}\right) + 0.006\varphi(T_4 - T_3) - (1.379\times10^{-6}\varphi - 2.970\times10^{-8}\mathrm{AF}_s)(T_4^2 - T_3^2) + (1.547\times10^{-10}\varphi + 0.636\times10^{-12}\mathrm{AF}_s)(T_4^3 - T_3^3)\right] - \frac{R(\varphi + 4.76a_s)}{\varphi M_f + M_a 4.76a_s}\left[\ln\left(\frac{T_4}{T_3}\right) + \ln(r_c)\right] = 0 \quad (19)$$

Besides, the total entropy change between points 2 and 3 (process $2 \rightarrow 3$) and between 4 and 1 (processes $4 \rightarrow 5$ and $5 \rightarrow 1$) is equal to zero [29,32]:

$$\Delta S_{2\rightarrow3} + \Delta S_{4\rightarrow5} + \Delta S_{5\rightarrow1} = 0 \quad (20)$$

By substituting the specific heat from Eqs. (7) and (14) and integrating from the initial to the final state of the process, the change in entropy in Eq. (20) can be written as

$$\frac{1}{\varphi+\mathrm{AF}_s}\left[(0.169\varphi + 0.913\mathrm{AF}_s)\ln\left(\frac{T_3T_1}{T_2T_4}\right) - (1.379\times10^{-6}\varphi - 2.970\times10^{-8}\mathrm{AF}_s)(T_1^2 - T_2^2 - T_4^2 + T_3^2) + (1.547\times10^{-10}\varphi + 0.636\times10^{-12}\mathrm{AF}_s)(T_1^3 - T_2^3 - T_4^3 + T_3^3) + 0.006\varphi(T_1 - T_2 - T_4 + T_3)\right] - \frac{R(\varphi + 4.76a_s)}{\varphi M_f + M_a 4.76a_s} \times \ln\left(\frac{T_3T_5}{T_2T_4}\right) = 0 \quad (21)$$

For an ideal cycle model, there are no losses. However, for a real internal combustion engine cycle, the heat transfer irreversibility between the working fluid and the cylinder wall and the friction-like term are not negligible [8,12,15,17]. The heat loss through the cylinder wall is assumed to be proportional to the average temperature of both the working fluid and the cylinder wall. So, the rate of heat loss can be evaluated as follows [8,34]:

$$\dot{Q}_{\mathrm{loss}} = \alpha_{\mathrm{conv}}A_{tr}(T_{\mathrm{avg}} - T_w) \quad (22)$$

where $\dot{Q}_{\mathrm{loss}}$ is the rate of heat loss, $\alpha_{\mathrm{conv}}$ is the heat-transfer coefficient, $A_{tr}$ is the area, $T_{\mathrm{avg}}$ is the average temperature of the working fluid, and $T_w$ is the average temperature of the cylinder wall. By substituting the heat-transfer coefficient, the average temperature of the working fluid, and the combustion chamber area into Eq. (22), the rate of heat loss can be calculated as follows:

$$\dot{Q}_{\mathrm{loss}} = 0.0625k\pi(D + 4L_{\mathrm{TDC}})\left[\frac{\rho_{\mathrm{air}}2LND}{\mu}\right]^{0.7}(T_3 + T_2 - 2T_w) \quad (23)$$

where $k$ is the thermal conductivity, $\mu$ is dynamic viscositym and $D$ is the piston diameter.

The total energy of the fuel per second input into the engine, of a gasoline-type fuel, can be expressed in terms of the equivalence ratio as [1]

$$\dot{Q}_{\mathrm{fuel}} = \eta_c\dot{m}_fQ_{\mathrm{LHV}} = \eta_{c\ \max}(-1.6082 + 4.6509/\varphi - 2.0746/\varphi^2)\dot{m}_fQ_{\mathrm{LHV}} \quad (24)$$

where $\dot{Q}_{\mathrm{fuel}}$ is the total heat released by combustion, $\eta_c$ is combustion efficiency, and $Q_{\mathrm{LHV}}$ is lower heating. The maximum possible value of the combustion efficiency $\eta_{c\ \max}$ is typically 0.9 in a spark ignition engine using a gasoline fuel. Thus, the rate of heat transferred to the working fluid by combustion during the process $2 \rightarrow 3$ can be represented by the following relation [33]:

$$\dot{Q}_{\text{in}} = \dot{Q}_{\text{fuel}} - \dot{Q}_{\text{loss}} = \frac{\eta_v \rho_{\text{air}} V_d N \varphi \eta_{c\ \max} Q_{\text{LHV}}}{2\text{AF}_s}(-1.6082 + 4.6509/\varphi - 2.0746/\varphi^2) - 0.0625k\pi(D + 4L_{\text{TDC}})\left[\frac{\rho_{\text{air}} 2LND}{\mu}\right]^{0.7}(T_3 + T_2 - 2T_w) \quad (25)$$

Every time the piston moves, friction acts to retard the motion [35–37]. Considering the friction effects on the piston in all the processes of the cycle, we assume a dissipation term represented by a friction force $F_\mu$ that is linearly proportional to the velocity of the piston [7–9], which can be written as follows:

$$F_f = -f\bar{\nu} \quad (26)$$

where $f$ is the coefficient of friction that takes into account the global losses on the power output, and $\nu$ is the piston's velocity. Running at engine speed $N$, the mean velocity of the piston is

$$\bar{\nu} = 2LN \quad (27)$$

where $L$ is the length stroke. In other words, $L$ is the total distance the piston travels per cycle.

Therefore, the power lost due to friction is [8]

$$P_f = F_f\bar{\nu} = -f\bar{\nu}^2 = -f(2LN)^2 \quad (28)$$

The power output of the Miller cycle engine is given by

$$P = \dot{Q}_{\text{in}} - \dot{Q}_{\text{out}} - P_f = \frac{\eta_v \rho_{\text{air}} V_d N(1 + \varphi/\text{AF}_s)}{2} \times \left\{\frac{1}{\varphi + \text{AF}_s}[(0.169\varphi + 0.913\text{AF}_s)(T_3 - T_2 - T_1 + T_4) + 0.003\varphi(T_3^2 - T_2^2 - T_1^2 + T_4^2) - (2.759 \times 10^{-6}\varphi - 5.941 \times 10^{-8}\text{AF}_s)(T_3^3 - T_2^3 - T_1^3 + T_4^3) + (4.643 \times 10^{-10}\varphi + 1.909 \times 10^{-12}\text{AF}_s)(T_3^4 - T_2^4 - T_1^4 + T_4^3)] - \frac{R(\varphi + 4.76a_s)(T_3 - T_2 - T_5 + T_4)}{\varphi M_f + M_a 4.76a_s}\right\} - f[L_2 N(r_c - 1)]^2 \quad (29)$$

The efficiency of the Miller cycle engine can be expressed by

$$\eta = \frac{P}{\dot{Q}_{\text{in}}} \times 100 = \frac{\frac{1}{\varphi+\text{AF}_s}[(0.169\varphi + 0.913\text{AF}_s)(T_3 - T_2 - T_1 + T_4) + 0.003\varphi(T_3^2 - T_2^2 - T_1^2 + T_4^2) - (2.759 \times 10^{-6}\varphi - 5.941 \times 10^{-8}\text{AF}_s)(T_3^3 - T_2^3 - T_1^3 + T_4^3) + (4.643 \times 10^{-10}\varphi + 1.909 \times 10^{-12}\text{AF}_s)(T_3^4 - T_2^4 - T_1^4 + T_4^3)] - \{[R(\varphi + 4.76a_s)(T_3 - T_2 - T_5 + T_4)]/(\varphi M_f + M_a 4.76a_s)\} - f[L_{\text{TDC}} N(r_c - 1)]^2}{\frac{1}{\varphi+\text{AF}_s}[0.003\varphi(T_3^2 - T_2^2) - (0.916 \times 10^{-6}\varphi + 1.980 \times 10^{-8}\text{AF}_s)(T_3^3 - T_2^3) + (1.160 \times 10^{-10}\varphi + 0.477 \times 10^{-12}\text{AF}_s)(T_3^4 - T_2^4) + (0.169\varphi + 0.913\text{AF}_s)(T_3 - T_2)] - \{[R(\varphi + 4.76a_s)(T_3 - T_2)]/(\varphi M_f + M_a 4.76a_s)\}} \times 100 \quad (30)$$

When $T_1$ is given, $T_2$ can be obtained from Eq. (18), then, substituting Eq. (15) by Eq. (25) yields $T_3$, and $T_4$ can be worked out by Eq. (19), and, the last, $T_5$ can be received from Eq. (21). Substituting $T_2$, $T_3$, $T_4$, and $T_5$ into Eqs. (29) and (30), respectively, the power output and thermal efficiency of the Miller cycle engine can be obtained.

## Numerical Example and Discussion

The following constants and parameter values have been used in this exercise: $D = 78.6$ mm, $L_{\alpha\beta} = 85$ mm, $T_1 = 300$ K, $N = 4000$ rpm, $T_w = 400$ K, $f = 12.9$ Nsm$^{-1}$, $x = 17$ mm, $\mu = 4.343$ kgk$^{-1}$ mol$^{-1}$, $k = 0.06763$ Wm$^{-1}$ K$^{-1}$, $M_a = 111$ kg kmol$^{-1}$, $M_f = 28.97$ kg kmol$^{-1}$, $Q_{\text{LHV}} = 44300$ kj kg$^{-1}$, $R = 8.314$ kj kg$^{-1}$ K$^{-1}$, $\phi = 1$, $\text{AF}_s = 15.1$, $\alpha_s = 12.5$, $\eta_v = 80\%$, and $r_c = 1 - 40$ [23–28,38–43]. The variable parameters in each case are given in Table 1. It should be noted that the variations of volume of piston displacement and volume of combustion chamber can be changed by the amount of the working fluid. Thus, in this work, two states are assumed in determining the amount of fluid working for each case:

1) First state: The amount of fluid working for each case is directly proportional to the piston displacement volume.

2) Second state: The amount of fluid working for all cases is proportional to the piston displacement volume in case A. Therefore, the amount of fluid working for all cases is the same.

Figures 2–5 show the power output versus compression ratio and the thermal efficiency versus compression ratio for the six cases of the Miller cycle. It can be concluded from these figures that the increase of compression ratio increases the power output at first and then decreases it. In other words, the power output versus compression ratio characteristic is approximately parabolic-like curves.

Figures 2 and 3 show the influence of the variation of combustion chamber volume and the variation of piston displacement volume on the Miller cycle performance. It should be noted here that, in Figs. 2 and 3, the amount of fluid working is proportional to the piston displacement volume for each case (first state). It can be observed in Figs. 2 and 3 that, if the compression ratio is less than a certain value, the power output and thermal efficiency increase with increasing piston displacement volume and remaining constant combustion chamber volume (comparison between cases A and B, and also between cases D and E). With further increase in the compression ratio, the power output and the thermal efficiency decrease with increasing piston displacement volume and remaining constant combustion chamber volume. It can be revealed that the maximum power output and the maximum efficiency increase and the working range of the cycle, the optimal compression ratio corresponding to the maximum power output point, and the optimal compression ratio corresponding to the maximum thermal efficiency point decrease

**Table 1 Variable parameter in each case in Fig. 1**

| Case | Effective compression ratio, $r_c^*$ | compression ratio, $r_c$ | Piston displacement volume, $V_d$ | Length stroke, $L$ | Position piston at TDC, $L_{\text{TDC}}$ |
|---|---|---|---|---|---|
| A | $(V_\alpha - V_L)/V_\beta$ | $V_\alpha/V_\beta$ | $V_{\alpha\beta}$ | $L_{\alpha\beta}$ | $L_\beta$ |
| B | $V_\alpha/V_\beta$ | $(V_\alpha + V_L)/V_\beta$ | $V_{\alpha\beta} + V_L$ | $L_{\alpha\beta} + x$ | $L_\beta$ |
| C | $(V_\alpha - 2V_L)/V_\beta$ | $(V_\alpha - V_L)/V_\beta$ | $V_{\alpha\beta} - V_L$ | $L_{\alpha\beta} - x$ | $L_\beta$ |
| D | $(V_\alpha - V_L)/(V_\beta - V_L)$ | $V_\alpha/(V_\beta - V_L)$ | $V_{\alpha\beta} + V_L$ | $L_{\alpha\beta} + x$ | $L_\beta - x$ |
| E | $V_\alpha/(V_\beta - V_L)$ | $(V_\alpha + V_L)/(V_\beta - V_L)$ | $V_{\alpha\beta} + 2V_L$ | $L_{\alpha\beta} + 2x$ | $L_\beta - x$ |
| F | $(V_\alpha - 2V_L)/(V_\beta - V_L)$ | $(V_\alpha - V_L)/(V_\beta - V_L)$ | $V_{\alpha\beta}$ | $L_{\alpha\beta}$ | $L_\beta - x$ |

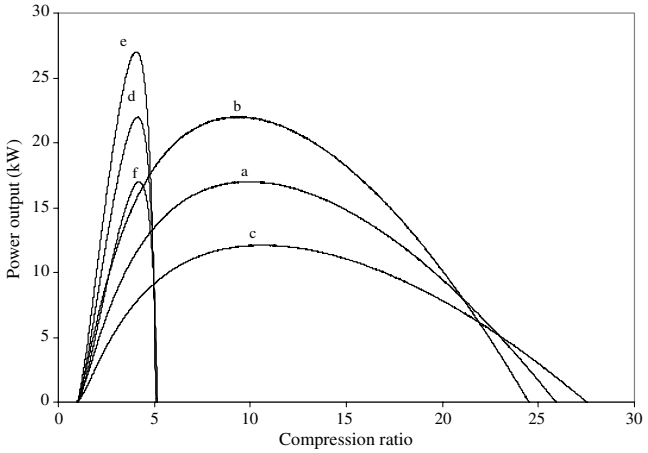


**Fig. 2 Power output versus compression ratio (amount of fluid working is proportional to the piston displacement volume for each case).**

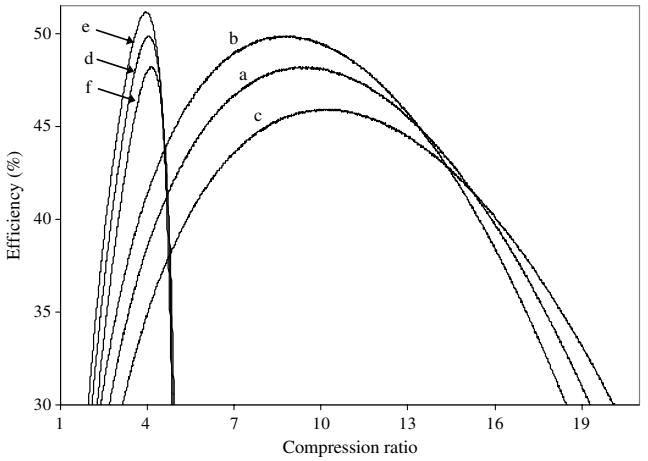


**Fig. 3 Thermal efficiency versus compression ratio (amount of fluid working is proportional to the piston displacement volume for each case).**

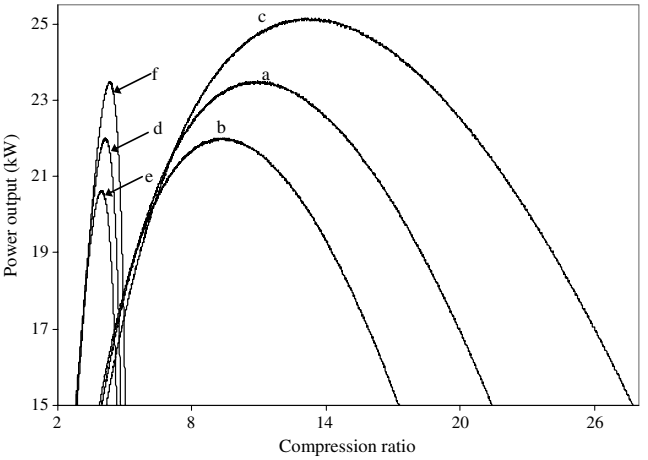


**Fig. 4 Power output versus compression ratio (amount of fluid working is similar for all cases).**

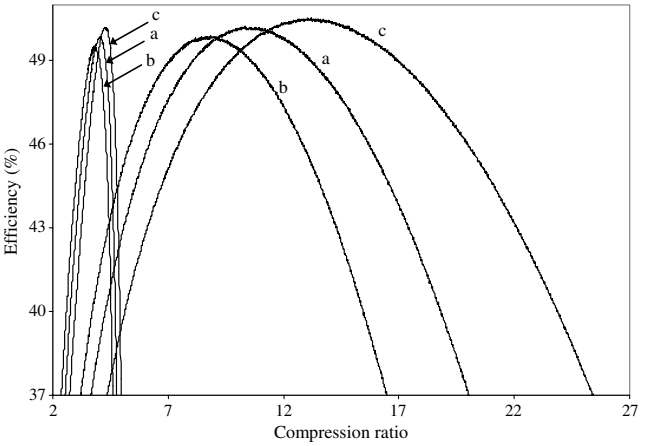


**Fig. 5 Power output versus compression ratio (amount of fluid working is similar for all cases).**

with increasing piston displacement volume and remaining constant combustion chamber volume.

Figures 4 and 5 indicate the influence of the variation of combustion chamber volume and piston displacement volume on the Miller cycle performance. It should be noted that, in Figs. 4 and 5, the amount of fluid working for all cases is the same (second state). The maximum power output and the maximum efficiency, the working range of the cycle, the optimal compression ratio corresponding to the maximum power output point, and the optimal compression ratio corresponding to the maximum thermal efficiency point increase with decreasing piston displacement volume and remaining constant combustion chamber volume (comparison between cases A and C, and also between cases D and F). As in these figures, if compression ratio is less than a certain value, the power output and thermal efficiency decrease with decreasing piston displacement volume and remaining constant combustion chamber volume, whereas if the compression ratio exceeds a certain value, the power output and thermal efficiency increase with decreasing piston displacement volume and remaining constant combustion chamber volume.

Figures 2–5, for both states, show that, if the compression ratio is less than a certain value, the power output and thermal efficiency increase with decreasing combustion volume, whereas if the compression ratio exceeds a certain value, the power output and thermal efficiency decrease with decreasing combustion volume. The optimal compression ratio corresponding to the maximum power output point, the optimal compression ratio corresponding to the maximum thermal efficiency point, and the working range of the cycle increase with decreasing combustion volume and the position of BDC remains constant (comparison between cases A and D, between cases B and E, and also between cases C and F). The maximum power output and the maximum efficiency in the first state increase and in the second state decrease with decreasing combustion volume and the position of BDC remains constant. The optimal compression ratio corresponding to the maximum power output point, the optimal compression ratio corresponding to the maximum thermal efficiency point, and the working range of the cycle decrease, whereas the maximum power output and the maximum efficiency remain constant with decreasing combustion volume and the piston displacement volume remains constant (comparison between cases A and F, and also between cases B and D).

## Conclusions

In this paper, the performance of a Miller cycle was analyzed by using finite time thermodynamics and the effects of variations of chamber combustion volume, piston displacement volume, and compression ratio on the power output and thermal efficiency of the Miller cycle were investigated by detailed numerical examples. The results obtained can be applied to the Otto, Atkinson, Diesel, and dual cycles. Thus, the results obtained are important to provide a good guidance for the performance evaluation and improvement of the practical internal combustion engine.

## References

[1] Stone, R., *Introduction to Internal Combustion Engines*, 3rd ed., Society of Automotive Engineers, Warrendale, PA, 1999, p. 641.

[2] Ribeiro, B., "Thermodynamic Optimization of Spark Ignition Engines at Part-Load Condition," Ph.D. Thesis, Univ. do Minho, Braga, Portugal, 2006.

[3] Kutlar, O. A., Arslan, H., and Calik-Tolga, A. T., "Methods to Improve Efficiency of Four Stroke, Spark Ignition Engines at Part Load," *Energy Conversion and Management*, Vol. 46, No. 20, 2005, pp. 3202–3220. doi:10.1016/j.enconman.2005.03.008

[4] Andresen, B., Berry, R. S., Ondrechen, M. J., and Salamon, P., "Thermodynamics for Processes in Finite Time," *Accounts of Chemical Research*, Vol. 17, No. 8, 1984, pp. 266–271. doi:10.1021/ar00104a001

[5] Ebrahimi, R., and Sherafati, M., "Thermodynamic Simulation of Performance of a Dual Cycle with Stroke Length and Volumetric Efficiency," *Journal of Thermal Analysis and Calorimetry*, Vol. 111, No. 1, 2013, pp. 951–957. doi:10.1007/s10973-012-2424-1

[6] Aragon-Gonzalez, G., Canales-Palma, A., and Leon-Galicia, A., "Maximum Irreversible Work and Efficiency in Power Cycles," *Journal of Physics D: Applied Physics*, Vol. 33, No. 11, 2000, pp. 1403–1409. doi:10.1088/0022-3727/33/11/321

[7] Verhas, J., "Thermodynamic Optimization of Finite-Time Processes (Book Review and the Authors' Answer to the Book Review)," *Journal of Thermal Analysis and Calorimetry*, Vol. 62, No. 3, 2000, pp. 873–881. doi:10.1023/A:1026706432022

[8] Ebrahimi, R., "Effects of Equivalence Ratio and Mean Piston Speed on Performance of an Irreversible Dual Cycle," *Acta Physica Polonica A*, Vol. 120, No. 3, 2011, pp. 384–389.

[9] Parlak, A., "Comparative Performance Analysis of Irreversible Dual and Diesel Cycles Under Maximum Power Conditions," *Energy Conversion and Management*, Vol. 46, No. 3, 2005, pp. 351–359. doi:10.1016/j.enconman.2004.04.001

[10] Ge, Y., Chen, L., Sun, F., and Wu, C., "Thermodynamic Simulation of Performance of an Otto Cycle with Heat Transfer and Variable Specific Heats for the Working Fluid," *International Journal of Thermal Sciences*, Vol. 44, No. 5, 2005, pp. 506–511. doi:10.1016/j.ijthermalsci.2004.10.001

[11] Pulkrabek, W. W., *Engineering Fundamental of the Internal Combustion Engine*, Prentice–Hall, Upper Saddle River, NJ, 1997, p. 425.

[12] Klein, S., "An Explanation for Observed Compression Ratios in Internal Combustion Engine," *Journal of Engineering for Gas Turbines and Power*, Vol. 113, No. 4, 1991, pp. 511–513. doi:10.1115/1.2906270

[13] Angulo-Brown, F., Fernandez-Betanzos, J., and Diaz-Pico, C. A., "Compression Ratio of an Optimized Air Standard Otto-Cycle Model," *European Journal of Physics*, Vol. 15, No. 1, 1994, pp. 38–42. doi:10.1088/0143-0807/15/1/007

[14] Al-Sarkhi, A., Akash, B. A., Jaber, J. O., Mohsen, M. S., and Abu-Nada, E., "Efficiency of Miller Engine at Maximum Power Density," *International Communications in Heat and Mass Transfer*, Vol. 29, No. 8, 2002, pp. 1159–1167. doi:10.1016/S0735-1933(02)00444-X

[15] Hou, S. S., "Heat Transfer Effects on the Performance of an Air Standard Dual Cycle," *Energy Conversion and Management*, Vol. 45, No. 18, 2004, pp. 3003–3015. doi:10.1016/j.enconman.2003.12.013

[16] Zhao, Y., and Chen, J., "Performance Analysis of an Irreversible Miller Heat Engine and Its Optimum Criteria," *Applied Thermal Engineering*, Vol. 27, No. 11, 2007, pp. 2051–2058. doi:10.1016/j.applthermaleng.2006.12.002

[17] Ge, Y., Chen, L., and Sun, F., "Finite-Time Thermodynamic Modeling and Analysis of an Irreversible Otto-Cycle," *Applied Energy*, Vol. 85, No. 7, 2007, pp. 618–624. doi:10.1016/j.apenergy.2007.09.008

[18] Al-Sarkhi, A., Al-Hinti, I., Abu-Nada, E., and Akash, B., "Performance Evaluation of Irreversible Miller Engine Under Various Specific Heat Models," *International Communications in Heat and Mass Transfer*, Vol. 34, No. 7, 2007, pp. 897–906. doi:10.1016/j.icheatmasstransfer.2007.03.012

[19] Wang, Y., Lin, L., Roskilly, A. P., Zeng, S., Huang, J., He, Y., Yunxin, H., Xiaodong, H., Huilan, H., Haiyan, W., Shangping, L., and Jing, Y., "An Analytic Study of Applying Miller Cycle to Reduce NOx Emission from Petrol Engine," *Applied Thermal Engineering*, Vol. 27, No. 11, 2007, pp. 1779–1789. doi:10.1016/j.applthermaleng.2007.01.013

[20] Wang, Y., Lin, L., Zeng, S., Huang, J., Roskilly, P., He, Y., Huang, X., and Li, S., "Application of the Miller Cycle to Reduce NOx Emissions from Petrol Engines," *Applied Energy*, Vol. 85, No. 6, 2008, pp. 463–474. doi:10.1016/j.apenergy.2007.10.009

[21] Chen, L. G., Ge, Y. L., and Sun, F. R., "Unified Thermodynamic Description and Optimization for a Class of Irreversible Reciprocating Heat Engine Cycles," *Proceedings of the Institution of Mechanical Engineers, Part D: Journal of Automobile Engineering*, Vol. 222, No. 8, 2008, pp. 1489–1500. doi:10.1243/09544070JAUTO827

[22] Lin, J. C., and Hou, S. S., "Performance Analysis of an Air-Standard Miller Cycle with Considerations of Heat Loss as Percentage of Fuel's Energy, Friction and Variable Specific Heat of Working Fluid," *International Journal of Thermal Sciences*, Vol. 47, No. 2, 2008, pp. 182–191. doi:10.1016/j.ijthermalsci.2007.02.002

[23] Ebrahimi, R., "Effects of Variable Specific Heat Ratio of Working Fluid on Performance of an Endoreversible Diesel Cycle," *Journal of the Energy Institute*, Vol. 83, No. 1, 2010, pp. 1–5. doi:10.1179/014426009X12519696923821

[24] Ebrahimi, R., "Effects of Mean Piston Speed, Equivalence Ratio and Cylinder Wall Temperature on Performance of an Atkinson Engine," *Mathematical and Computer Modeling*, Vol. 53, Nos. 5–6, 2010, pp. 1289–1297. doi:10.1016/j.mcm.2010.12.015

[25] Wang, Y., Zeng, S., Huang, J., He, Y., Huang, X., Lin, L., and Li, S., "Experimental Investigation of Applying Miller Cycle to Reduce NOx Emissions From Diesel Engine," *Proceedings of the Institution of Mechanical Engineers*, Vol. 219, No. 5, 2005, pp. 631–638. doi:10.1243/095765005X31289

[26] Anderson, M. K., Assanis, D. S., and Filipi, Z., "First and Second Law Analyses of a Naturally-Aspirated, Miller Cycle, SI Engine with Late Intake Valve Closure," Society of Automotive Engineers Paper 980889, 1998.

[27] Ribeiro, B., and Martins, J., "Thermodynamic Analysis of Spark Ignition Engines Using the Entropy Generation Minimisation Method," *International Journal of Exergy*, Vol. 6, No. 1, 2009, pp. 93–109. doi:10.1504/IJEX.2009.023347

[28] Heywood, J. B., *Internal Combustion Engine Fundamentals*, McGraw–Hill, New York, 1988, p. 930.

[29] Cengel, Y. A., and Boles, M. A., *Thermodynamic Engineering Approach*, 3rd ed., McGraw–Hill, New York, 1998, p. 1010.

[30] Ferguson, C., and Kirkpatric, A., *Internal Combustion Engine: Applied Thermosciences*, Wiley, New York, 2001, p. 369.

[31] McBride, B., Gordan, S., and Reno, M., "Coefficients for Calculating Thermodynamic and Transport Properties of Individual Species," NASA TM-4513, 1993.

[32] Al-Sarkhi, A., Jaber, J. O., and Probert, S. D., "Efficiency of Miller Engine," *Applied Energy*, Vol. 83, No. 4, 2006, pp. 343–359. doi:10.1016/j.apenergy.2005.04.003

[33] Ebrahimi, R., "Effects of Variable Specific Heat Ratio on Performance of an Endoreversible Otto Cycle," *Acta Physica Polonica*, Vol. 117, No. 6, 2010, pp. 887–891.

[34] Al-Hinit, I., Akash, B., Abu-Nada, E., and Al-Sarkhi, A., "Performance Analysis of Air-Standard Diesel Cycle Using an Alternative Irreversible Heat Transfer Approach," *Energy Conversion and Management*, Vol. 49, No. 11, 2008, pp. 3301–3304. doi:10.1016/j.enconman.2007.10.034

[35] Mozurkewich, M., and Berry, R. S., "Optimal Paths for Thermodynamic System: The Ideal Otto Cycle," *Applied Physics*, Vol. 54, No. 77, 1981, pp. 3651–3661. doi:10.1063/1.329894

[36] Hoffman, K. H., Watowich, S. J., and Berry, R. S., "Optimal Paths for Thermodynamic System: The Ideal Diesel Cycle," *Applied Physics*, Vol. 58, No. 6, 1985, pp. 2125–2134. doi:10.1063/1.335977

[37] Qin, X., Chen, L., Sun, F., and Wu, C., "The Universal Power and Efficiency Characteristics for Irreversible Reciprocating Heat Engine Cycles," *European Journal of Physics*, Vol. 24, No. 4, 2003, pp. 1–8. doi:10.1088/0143-0807/24/4/354

[38] Ge, Y., Chen, L., Sun, F., and Wu, C., "Effects of Heat Transfer and Friction on the Performance of an Irreversible Air-Standard Miller Cycle," *International Communications in Heat and Mass Transfer*, Vol. 32, No. 8, 2005, pp. 1045–1056. doi:10.1016/j.icheatmasstransfer.2005.02.002

[39] Ge, Y., Chen, L., Sun, F., and Wu, C., "Effects of Heat Transfer and Variable Specific Heats of Working Fluid on Performance of a Miller Cycle," *International Journal of Ambient Energy*, Vol. 26, No. 4, 2005, pp. 203–214. doi:10.1080/01430750.2005.9674991

[40] Chen, L., Ge, Y., and Sun, F., "The Performance of a Miller Cycle with Heat Transfer, Friction and Variable Specific Heats of Working Fluid," *Termotehnica*, Vol. 14, No. 2, 2010, pp. 24–32.

[41] Liu, J., and Chen, J., "Optimum Performance Analysis of a Class of Typical Irreversible Heat Engines with Temperature-Dependent Heat Capacities of the Working Substance," *International Journal of Ambient Energy*, Vol. 31, No. 2, 2010, pp. 59–70. doi:10.1080/01430750.2010.9675103

[42] Chen, L., Ge, Y., and Sun, F., "Finite Time Thermodynamic Modeling and Analysis for an Irreversible Miller Cycle," *International Journal of Ambient Energy*, Vol. 32, No. 2, 2011, pp. 87–94. doi:10.1080/01430750.2011.584457

[43] Yasar, H., "First and Second Law Analysis of Low Heat Rejection Diesel Engine," *Journal of the Energy Institute*, Vol. 81, No. 1, 2008, pp. 48–53. doi:10.1179/174602208X269544